

LA-UR-15-21365

Approved for public release; distribution is unlimited.

Title: Uncertainties of the Y_n Parameters of the Hage-Cifarelli Formalism

Author(s): Smith-Nelson, Mark A.
 Burr, Thomas Lee
 Hutchinson, Jesson D.
 Cutler, Theresa Elizabeth

Intended for: Report

Issued: 2015-08-14 (rev.1)

Disclaimer:

Los Alamos National Laboratory, an affirmative action/equal opportunity employer, is operated by the Los Alamos National Security, LLC for the National Nuclear Security Administration of the U.S. Department of Energy under contract DE-AC52-06NA25396. By approving this article, the publisher recognizes that the U.S. Government retains nonexclusive, royalty-free license to publish or reproduce the published form of this contribution, or to allow others to do so, for U.S. Government purposes. Los Alamos National Laboratory requests that the publisher identify this article as work performed under the auspices of the U.S. Department of Energy. Los Alamos National Laboratory strongly supports academic freedom and a researcher's right to publish; as an institution, however, the Laboratory does not endorse the viewpoint of a publication or guarantee its technical correctness.

Uncertainties of the Y_n Parameters of the Hage-Cifarelli Formalism

Application Note

Mark Smith-Nelson, Thomas Burr, Jesson Hutchinson, Theresa Cutler

Introduction

One method for determining the physical parameters of a multiplying system is summarized by Cifarelli [1]. In this methodology the single, double and triple rates are determined from what is commonly referred to as Feynman histograms. This paper will examine two methods for estimating the uncertainty in the parameters used in inferring these rates. These methods will be compared with simulated data in order to determine which one best approximates the sample uncertainty.

This paper concentrates on the uncertainties in the first three multiplicity rates and the parameters associated with them. Terms associated with the quads rates are presented sparingly to reduce transcription errors.

The intent of this paper is to serve as a reference for those already familiar with creating Feynman histograms and the Hage-Cifarelli formalism.

Moments of a histogram

The common equations for the moments of a histogram [2] will be referred to in this paper as the standard moments. These are the moments used in Robba [3] and the first four moments are calculated by

$$\overline{C_1} = \frac{\sum_{k=0}^K k c_k}{\sum_{k=0}^K c_k}, \quad (1)$$

$$\overline{C_2} = \frac{\sum_{k=0}^K k^2 c_k}{\sum_{k=0}^K c_k}, \quad (2)$$

$$\overline{C_3} = \frac{\sum_{k=0}^K k^3 c_k}{\sum_{k=0}^K c_k}, \text{ and} \quad (3)$$

$$\overline{C_4} = \frac{\sum_{k=0}^K k^4 c_k}{\sum_{k=0}^K c_k} \quad (4)$$

where c_k is the number of counts in the bin k of a histogram.

However, the moments used in the Hage-Cifarelli formalism are not the standard moments and will be referred to as the reduced factorial moments [4]. The first four reduced factorial moments are calculated by

$$\overline{m_1} = \frac{\sum_{k=0}^K k c_k}{1! \sum_{k=0}^K c_k}, \quad (5)$$

$$\overline{m_2} = \frac{\sum_{k=0}^K k(k-1) c_k}{2! \sum_{k=0}^K c_k}, \quad (6)$$

$$\overline{m_3} = \frac{\sum_{k=0}^K k(k-1)(k-2) c_k}{3! \sum_{k=0}^K c_k}, \text{ and} \quad (7)$$

$$\overline{m_4} = \frac{\sum_{k=0}^K k(k-1)(k-2)(k-3) c_k}{4! \sum_{k=0}^K c_k}. \quad (8)$$

In one of the steps of the uncertainty derivations the factors are expressed in terms of the standard moments. For convenience it is desired to convert the standard moments to the reduced factorial moments. The identities between the standard and reduced factorial moments are given below in Table 1 and Table 2.

Table 1. Representation of the reduced factorial moments in terms of the standard moments.

$\overline{m}_1 = \overline{C}_1$	
$\overline{m}_2 = \frac{\overline{C}_2 - \overline{C}_1}{2}$	
$\overline{m}_3 = \frac{\overline{C}_3 - 3\overline{C}_2 + 2\overline{C}_1}{6}$	
$\overline{m}_4 = \frac{\overline{C}_4 - 6\overline{C}_3 + 11\overline{C}_2 - 6\overline{C}_1}{24}$	
$\overline{m}_5 = \frac{\overline{C}_5 - 10\overline{C}_4 + 35\overline{C}_3 - 50\overline{C}_2 + 24\overline{C}_1}{5!}$	5! = 120
$\overline{m}_6 = \frac{\overline{C}_6 - 15\overline{C}_5 + 85\overline{C}_4 - 225\overline{C}_3 + 274\overline{C}_2 - 120\overline{C}_1}{6!}$	6! = 720
$\overline{m}_7 = \frac{\overline{C}_7 - 21\overline{C}_6 + 175\overline{C}_5 - 735\overline{C}_4 + 1624\overline{C}_3 - 1764\overline{C}_2 + 720\overline{C}_1}{7!}$	7! = 5040
$\overline{m}_8 = \frac{\overline{C}_8 - 28\overline{C}_7 + 322\overline{C}_6 - 1960\overline{C}_5 + 6769\overline{C}_4 - 13132\overline{C}_3 + 13068\overline{C}_2 - 5040\overline{C}_1}{8!}$	8! = 40320

Table 2. Representation of the standard moments in terms of the reduced factorial moments.

$\overline{C}_1 = \overline{m}_1$
$\overline{C}_2 = 2\overline{m}_2 + \overline{m}_1$
$\overline{C}_3 = 6\overline{m}_3 + 6\overline{m}_2 + \overline{m}_1$
$\overline{C}_4 = 24\overline{m}_4 + 36\overline{m}_3 + 14\overline{m}_2 + \overline{m}_1$
$\overline{C}_5 = \overline{m}_1 + 30\overline{m}_2 + 150\overline{m}_3 + 240\overline{m}_4 + 120\overline{m}_5$
$\overline{C}_6 = \overline{m}_1 + 62\overline{m}_2 + 540\overline{m}_3 + 1560\overline{m}_4 + 1800\overline{m}_5 + 720\overline{m}_6$
$\overline{C}_7 = \overline{m}_1 + 126\overline{m}_2 + 1806\overline{m}_3 + 8400\overline{m}_4 + 16800\overline{m}_5 + 15120\overline{m}_6 + 5040\overline{m}_7$
$\overline{C}_8 = \overline{m}_1 + 254\overline{m}_2 + 5796\overline{m}_3 + 40824\overline{m}_4 + 126000\overline{m}_5 + 191520\overline{m}_6 + 141120\overline{m}_7 + 40320\overline{m}_8$

The method for deriving the uncertainties of the reduced factorial moments is presented in Burr and Smith-Nelson [5]. The starting equations for the variance of the reduced factorial moments are

$$\sigma_{\overline{m_1}}^2 = \frac{1}{N-1} \frac{\sum_{k=0}^K \left(k - \overline{m_1} \right)^2 c_k}{\sum_{k=0}^K c_k}, \quad (9)$$

$$\sigma_{\overline{m_2}}^2 = \frac{1}{N-1} \frac{\sum_{k=0}^K \left(\frac{k(k-1)}{2!} - \overline{m_2} \right)^2 c_k}{\sum_{k=0}^K c_k}, \quad (10)$$

$$\sigma_{\overline{m_3}}^2 = \frac{1}{N-1} \frac{\sum_{k=0}^K \left(\frac{k(k-1)(k-2)}{3!} - \overline{m_3} \right)^2 c_k}{\sum_{k=0}^K c_k}, \text{ and} \quad (11)$$

$$\sigma_{\overline{m_4}}^2 = \frac{1}{N-1} \frac{\sum_{k=0}^K \left(\frac{k(k-1)(k-2)(k-3)}{4!} - \overline{m_4} \right)^2 c_k}{\sum_{k=0}^K c_k} \quad (12)$$

where N is the number of gates in the histogram. For histograms generated for multiplication calculations N can be calculated by

$$N = \sum_{k=0}^K c_k. \quad (13)$$

The resulting equations for the variances are

$$\sigma_{\overline{m_1}}^2 = \frac{2\overline{m_2} + \overline{m_1} - \overline{m_1}^2}{N-1}, \quad (14)$$

$$\sigma_{\overline{m_2}}^2 = \frac{6\overline{m_4} + 6\overline{m_3} + \overline{m_2} - \overline{m_2}^2}{N-1}, \quad (15)$$

$$\sigma_{\overline{m_3}}^2 = \frac{20\overline{m_6} + 30\overline{m_5} + 12\overline{m_4} + \overline{m_3} - \overline{m_3}^2}{N-1}, \text{ and} \quad (16)$$

$$\sigma_{\overline{m_4}}^2 = \frac{70\overline{m_8} + 140\overline{m_7} + 90\overline{m_6} + 20\overline{m_5} + \overline{m_4} - \overline{m_4}^2}{N-1}. \quad (17)$$

Example Histogram

For illustration, an example histogram is presented in Table 3 and the data are plotted in Figure 1. The reduced factorial moments and uncertainties for the example histogram are presented in Table 4.

Table 3. The values of the histogram used for illustration purposes.

k	c_k
0	8
1	26
2	64
3	120
4	176
5	199
6	176
7	120
8	64
9	26
10	8
11	2
12	0
Number of gates (N)	989

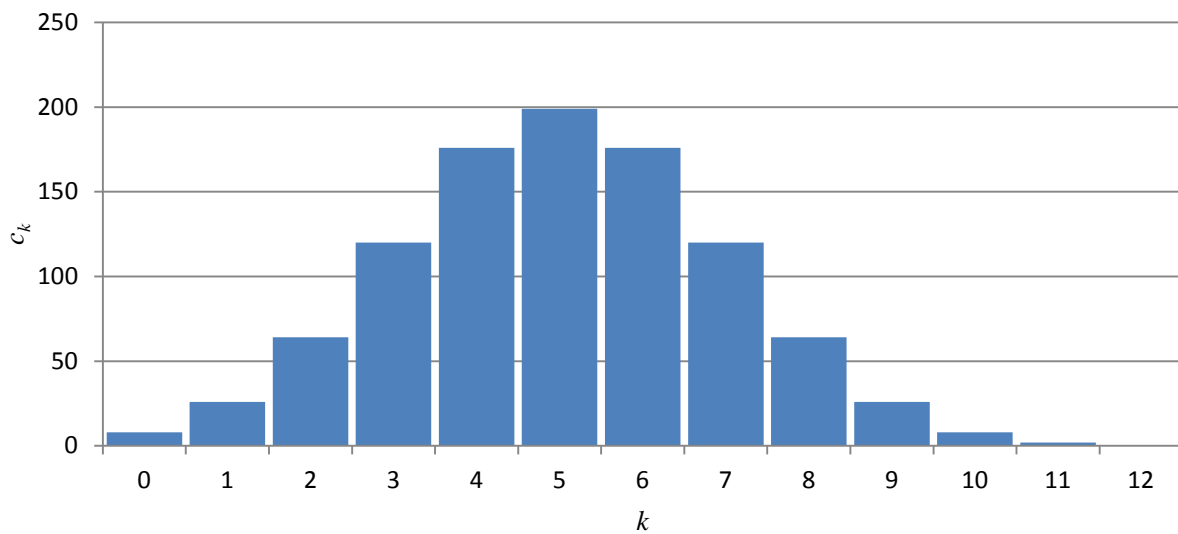


Figure 1. An example histogram used for illustrating the parameters in the uncertainty estimation.

Table 4. The reduced factorial moments of the example histogram and the associated uncertainties.

Moment	Value	% Uncertainty
$\overline{m_1}$	5.012 \pm 0.062	1.2 %
$\overline{m_2}$	11.960 \pm 0.294	2.5 %
$\overline{m_3}$	17.788 \pm 0.702	3.9 %
$\overline{m_4}$	18.308 \pm 1.088	5.9 %
$\overline{m_5}$	13.726 \pm 1.206	8.8 %
$\overline{m_6}$	7.680 \pm 0.992	12.9 %

Feynman Histograms

The intention of this paper is to examine the uncertainty associated with Feynman histograms and to act as a reference. Therefore, only a very brief explanation of Feynman histograms is presented.

For multiplicity measurements neutron events are time-tagged as to when they are detected and stored in a file. During post processing, multiple gates of width τ , which are typically on the order of a few microseconds, are “opened” and the number of events in the gate are counted. The number of events in each gate are then binned into a histogram. This process is repeated for multiple gatewidths and results in multiple Feynman histograms. In the above example histogram and throughout this paper k is the number of events detected in a gate and c_k is the number of times k events were detected in a gate. A more detailed explanation of generating Feynman histograms can be found in Cutler [6].

In this paper the start of the gates is determined randomly. It is important to note that there is no guarantee that each individual event will be used only once. This method is commonly referred to as the bootstrap method and was demonstrated in Burr and Smith-Nelson [5] to give accurate estimations of the uncertainty in the first and second reduced factorial moments of a Feynman histogram.

The single, double, triple, and quad rates are calculated by fitting the Y_n parameters [1][7] and finding the asymptote. The parameters Y_1 , Y_2 , Y_3 , and Y_4 are calculated by

$$Y_1 = \frac{\overline{m_1}}{\tau}, \quad (18)$$

$$Y_2 = \frac{1}{\tau} \left(\overline{m_2} - \frac{1}{2} \overline{m_1}^2 \right), \quad (19)$$

$$Y_3 = \frac{1}{\tau} \left(\overline{m_3} - \overline{m_2} \overline{m_1} + \frac{1}{3} \overline{m_1}^3 \right), \text{ and} \quad (20)$$

$$Y_4 = \frac{1}{\tau} \left(\overline{m_4} - \overline{m_3} \overline{m_1} + \overline{m_2} \overline{m_1}^2 - \frac{1}{2} \overline{m_2}^2 - \frac{1}{4} \overline{m_1}^4 \right). \quad (21)$$

Sum of Differences Method

The Y_n parameters are used in determining the multiplicity rates and we are interested in determining the uncertainty in Y_n . The first method proposed follows the same premise as stated in equations (9) through (12) above. This method is presented in Richard [8] and Verbeke [9]. It is appropriate to point out that Verbeke extends the uncertainty estimation for the fractional Y_n 's in a different manner. His estimation of the uncertainties associated with the fractional Y_n 's show good agreement with his simulations as well. The fractional Y_n uncertainties are presented at the end of this paper.

The derivations using the sum of differences methods start with

$$\delta_{Y_1}^2 = \frac{\sum_{k=0}^K \left(\frac{k}{\tau} - Y_1 \right)^2 c_k}{(N-1) \sum_{k=0}^K c_k}, \quad (22)$$

$$\delta_{Y_2}^2 = \frac{\sum_{k=0}^K \left(\frac{1}{\tau} \left(\frac{k(k-1)}{2!} - \frac{1}{2} \overline{m_1^2} \right) - Y_2 \right)^2 c_k}{(N-1) \sum_{k=0}^K c_k}, \text{ and} \quad (23)$$

$$\delta_{Y_3}^2 = \frac{\sum_{k=0}^K \left(\frac{1}{\tau} \left(\frac{k(k-1)(k-2)}{3!} - \frac{k(k-1)}{2!} \overline{m_1} + \frac{1}{3} \overline{m_1^3} \right) - Y_3 \right)^2 c_k}{(N-1) \sum_{k=0}^K c_k}. \quad (24)$$

The resulting equations are

$$\delta_{Y_1} = \frac{\sqrt{2\overline{m_2} + \overline{m_1} - \overline{m_1^2}}}{\sqrt{N-1} \times \tau}, \quad (25)$$

$$\delta_{Y_2} = \frac{\sqrt{6\overline{m_4} + 6\overline{m_3} + \overline{m_2} - \overline{m_2^2}}}{\sqrt{N-1} \times \tau}, \text{ and} \quad (26)$$

$$\delta_{Y_3} = \frac{\sqrt{\begin{pmatrix} 20\overline{m_6} + 30\overline{m_5} + 12\overline{m_4} + \overline{m_3} - \overline{m_3^2} - 20\overline{m_5 m_1} \\ -24\overline{m_4 m_1} + 6\overline{m_4 m_1^2} - 6\overline{m_3 m_1} + 6\overline{m_3 m_1^2} \\ + \overline{m_2 m_1^2} - \overline{m_2^2 m_1} + 2\overline{m_3 m_2 m_1} \end{pmatrix}}}{\sqrt{N-1} \times \tau}. \quad (27)$$

The solutions for δ_{Y_4} were not calculated because the result is long and prone to transcription errors. Also, one will see that deriving δ_{Y_4} will not be needed.

Propagation of Uncertainties Method

Another method for estimating the uncertainty can be done by the standard propagation of uncertainties of the Y_n parameters and is presented in Burr and Butterfield [10], Mattingly [11], Robba [3] and Okowita [12]. The extended algebraic manipulations in this paper were performed using Maple™ ver. 14.0 [13]. Maple™ is a symbolic mathematical solver and is good for “brute force” calculations. However, Maple™ is not good at formatting results for print. To avoid transcription errors the final results of terms associated with quads are presented here but intermediary steps are omitted. The starting equations for the variances are

$$\sigma_{Y_1}^2 = \left(\frac{\partial Y_1}{\partial m_1} \right)^2 \sigma_{m_1}^2, \quad (28)$$

$$\sigma_{Y_2}^2 = \left(\frac{\partial Y_2}{\partial m_1} \right)^2 \sigma_{m_1}^2 + \left(\frac{\partial Y_2}{\partial m_2} \right)^2 \sigma_{m_2}^2 + 2 \frac{\partial Y_2}{\partial m_1} \frac{\partial Y_2}{\partial m_2} \sigma_{m_1 m_2}, \quad (29)$$

$$\sigma_{Y_3}^2 = \left(\begin{aligned} &\left(\frac{\partial Y_3}{\partial m_1} \right)^2 \sigma_{m_1}^2 + \left(\frac{\partial Y_3}{\partial m_2} \right)^2 \sigma_{m_2}^2 + \left(\frac{\partial Y_3}{\partial m_3} \right)^2 \sigma_{m_3}^2 \\ &+ 2 \frac{\partial Y_3}{\partial m_1} \frac{\partial Y_3}{\partial m_2} \sigma_{m_1 m_2} + 2 \frac{\partial Y_3}{\partial m_1} \frac{\partial Y_3}{\partial m_3} \sigma_{m_1 m_3} + 2 \frac{\partial Y_3}{\partial m_2} \frac{\partial Y_3}{\partial m_3} \sigma_{m_2 m_3} \end{aligned} \right), \text{ and} \quad (30)$$

$$\sigma_{Y_4}^2 = \left(\begin{aligned} &\left(\frac{\partial Y_4}{\partial m_1} \right)^2 \sigma_{m_1}^2 + \left(\frac{\partial Y_4}{\partial m_2} \right)^2 \sigma_{m_2}^2 + \left(\frac{\partial Y_4}{\partial m_3} \right)^2 \sigma_{m_3}^2 + \left(\frac{\partial Y_4}{\partial m_4} \right)^2 \sigma_{m_4}^2 \\ &+ 2 \frac{\partial Y_4}{\partial m_1} \frac{\partial Y_4}{\partial m_2} \sigma_{m_1 m_2} + 2 \frac{\partial Y_4}{\partial m_1} \frac{\partial Y_4}{\partial m_3} \sigma_{m_1 m_3} + 2 \frac{\partial Y_4}{\partial m_1} \frac{\partial Y_4}{\partial m_4} \sigma_{m_1 m_4} \\ &+ 2 \frac{\partial Y_4}{\partial m_2} \frac{\partial Y_4}{\partial m_3} \sigma_{m_2 m_3} + 2 \frac{\partial Y_4}{\partial m_2} \frac{\partial Y_4}{\partial m_4} \sigma_{m_2 m_4} \\ &+ 2 \frac{\partial Y_4}{\partial m_3} \frac{\partial Y_4}{\partial m_4} \sigma_{m_3 m_4} \end{aligned} \right). \quad (31)$$

Where the covariance terms associated with the first three moments are calculated by

$$\sigma_{\overline{m_1 m_2}} = \frac{1}{N-1} \frac{\sum_{k=0}^K \left(k - \overline{m_1} \right) \left(\frac{k(k-1)}{2!} - \overline{m_2} \right) c_k}{\sum_{k=0}^K c_k}, \quad (32)$$

$$\sigma_{\overline{m_1 m_3}} = \frac{1}{N-1} \frac{\sum_{k=0}^K \left(k - \overline{m_1} \right) \left(\frac{k(k-1)(k-2)}{3!} - \overline{m_3} \right) c_k}{\sum_{k=0}^K c_k}, \text{ and} \quad (33)$$

$$\sigma_{\overline{m_2 m_3}} = \frac{1}{N-1} \frac{\sum_{k=0}^K \left(\frac{k(k-1)}{2!} - \overline{m_2} \right) \left(\frac{k(k-1)(k-2)}{3!} - \overline{m_3} \right) c_k}{\sum_{k=0}^K c_k}. \quad (34)$$

The terms associated with the quads are calculated in similar fashion.

The resulting variances in terms of reduced factorial moments are

$$\sigma_{Y_1} = \frac{\sqrt{2\overline{m_2} + \overline{m_1} - \overline{m_1}^2}}{\sqrt{N-1} \times \tau}, \quad (35)$$

$$\sigma_{Y_2} = \frac{\sqrt{6\overline{m_4} + 6\overline{m_3} + \overline{m_2} - \overline{m_2}^2 + 4\overline{m_2 m_1}^2 + \overline{m_1}^3 - \overline{m_1}^4 - 6\overline{m_3 m_1} - 4\overline{m_2 m_1}}}{\sqrt{N-1} \times \tau}, \quad (36)$$

$$\sigma_{Y_3} = \frac{\sqrt{\begin{pmatrix} 20\overline{m_6} + 30\overline{m_5} + 12\overline{m_4} + \overline{m_3} - \overline{m_3}^2 + 2\overline{m_2}^3 + \overline{m_1}^5 - \overline{m_1}^6 - 20\overline{m_5 m_1} \\ -8\overline{m_4 m_2} - 24\overline{m_4 m_1} + 14\overline{m_4 m_1}^2 - 6\overline{m_3 m_2} - 6\overline{m_3 m_1} + 12\overline{m_3 m_1}^2 - 8\overline{m_3 m_1}^3 \\ + 5\overline{m_2}^2 \overline{m_1} + \overline{m_2 m_1}^2 - 6\overline{m_2 m_1}^3 + 6\overline{m_2 m_1}^4 - 8\overline{m_2}^2 \overline{m_1}^2 + 10\overline{m_3 m_2 m_1} \end{pmatrix}}}{\sqrt{N-1} \times \tau}, \text{ and} \quad (37)$$

$$\sigma_{Y_4} = \frac{\sqrt{\begin{pmatrix} 70\overline{m_8} + 140\overline{m_7} + 90\overline{m_6} + 20\overline{m_5} + \overline{m_4} - \overline{m_4}^2 + \overline{m_2}^3 - \overline{m_2}^4 + \overline{m_1}^7 - \overline{m_1}^8 \\ -70\overline{m_7 m_1} + 50\overline{m_6 m_1}^2 - 120\overline{m_6 m_1} - 10\overline{m_5 m_3} + 70\overline{m_5 m_1}^2 - 30\overline{m_5 m_1}^3 \\ + 12\overline{m_4 m_3 m_1} + 40\overline{m_4 m_2 m_1} - 40\overline{m_5 m_2} - 30\overline{m_6 m_2} - 60\overline{m_5 m_1} + 40\overline{m_5 m_2 m_1} \\ - 8\overline{m_4 m_3} - 12\overline{m_4 m_2} - 8\overline{m_4 m_1} + 16\overline{m_4 m_1}^4 + 8\overline{m_4 m_2}^2 + 24\overline{m_4 m_1}^2 - 32\overline{m_4 m_1}^3 \\ - 34\overline{m_4 m_2 m_1}^2 - 24\overline{m_3 m_2} \overline{m_1} - 32\overline{m_3 m_2 m_1}^2 - 6\overline{m_3 m_1}^3 + 8\overline{m_3}^2 \overline{m_2} \\ + 7\overline{m_3}^2 \overline{m_1} - 10\overline{m_3}^2 \overline{m_1}^2 + 14\overline{m_3 m_1}^4 - 10\overline{m_3 m_1}^5 + 10\overline{m_3 m_2}^2 + \overline{m_3 m_1}^2 \\ - 2\overline{m_2}^2 \overline{m_1}^2 + \overline{m_2 m_1}^4 + 14\overline{m_2}^3 \overline{m_1}^2 + 16\overline{m_2}^2 \overline{m_1}^3 - 19\overline{m_2}^2 \overline{m_1}^4 - 8\overline{m_2 m_1}^5 \\ + 8\overline{m_2 m_1}^6 + 34\overline{m_3 m_2 m_1}^3 + 6\overline{m_3 m_2 m_1} - 8\overline{m_2}^3 \overline{m_1} \end{pmatrix}}}{\sqrt{N-1} \times \tau}. \quad (38)$$

The covariances are simplified to

$$\sigma_{\overline{m_1 m_2}} = \frac{3\overline{m_3} + 2\overline{m_2} - \overline{m_1 m_2}}{N-1}, \quad (39)$$

$$\sigma_{\overline{m_1 m_3}} = \frac{4\overline{m_4} + 3\overline{m_3} - \overline{m_1 m_3}}{N-1}, \text{ and} \quad (40)$$

$$\sigma_{\overline{m_2 m_3}} = \frac{10\overline{m_5} + 12\overline{m_4} + 3\overline{m_3} - \overline{m_2 m_3}}{N-1}. \quad (41)$$

The terms associated with the fourth moments are not presented here to avoid transcription errors.

It is good to note here the difference in notation for the two versions of uncertainty. For this paper δ_{Y_n} , equations (22) to (27), correspond to the uncertainty calculated by the sum of differences method and σ_{Y_n} , equations (28) to (41), correspond to the uncertainty calculated by the standard propagation of uncertainties for Y_n .

Comparison of Uncertainties

The two methods presented give different equations for estimating the uncertainty in Y_n . To determine which method best approximates the uncertainty of multiple samples, monte-carlo simulations of neutron chains were performed [14].

One hundred (100) simulations were generated with characteristics emulating a 4.5 kg sphere of alpha-phase plutonium. Five hundred and twelve (512) Feynman histograms were generated for each simulation where the gatewidths ranged from 4 μs to 2048 μs . The start time of the gates was randomly chosen [6] and it is important to note there was a possibility that events may be used multiple times. The number of gates was not kept constant for each gatewidth. Rather the number of gates for each gatewidth was determined by

$$\text{number of Gates} = 0.8 \frac{\text{Total Count Time}}{\text{Gatewidth}}.$$

The Y_1 , Y_2 , and Y_3 parameters were calculated for each gatewidth of the 100 simulations and plotted in Figure 2, Figure 3, and Figure 4 along with the calculated uncertainties. These figures show that σ_{Y_n} is a better estimator of the uncertainty than δ_{Y_n} . This can be seen because δ_{Y_n} diverges significantly at larger gatewidths while σ_{Y_n} is closer to the spread of the data points in the multiple simulations.

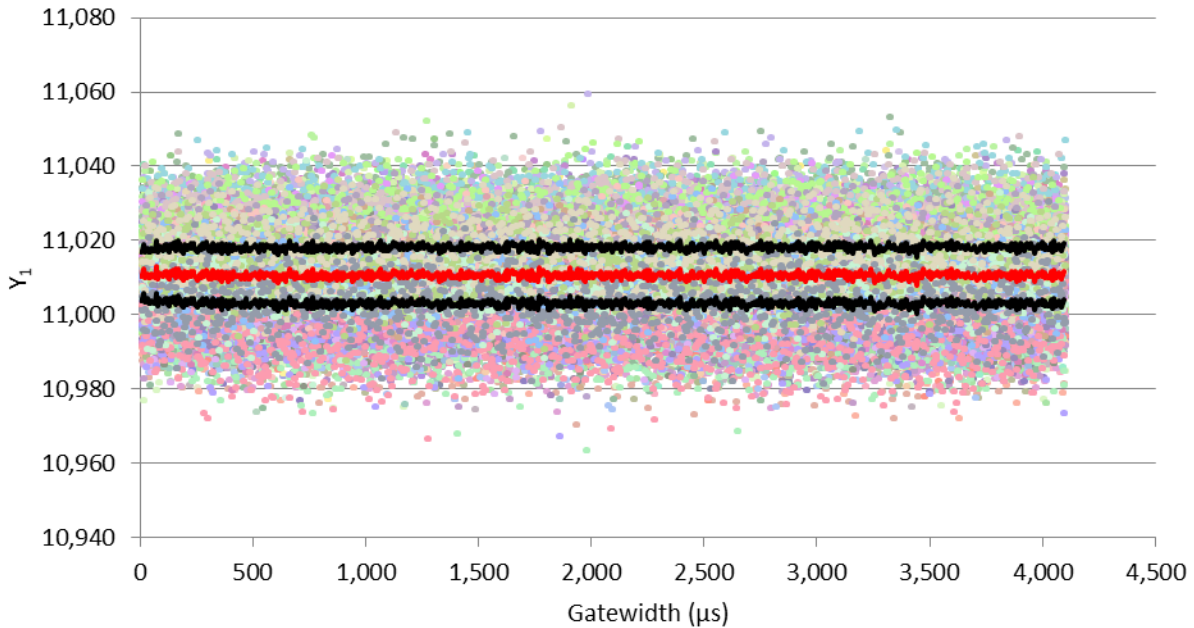


Figure 2. Estimation of Y_1 parameter for each gatewidth for a simulation of a 4.5 kg sphere of plutonium. The red center line is the average value for Y_1 for each gatewidth while the black line is the uncertainty calculated by σ_{Y_1} for each gatewidth. Note, for Y_1 , $\sigma_{Y_1} = \delta_{Y_1}$.

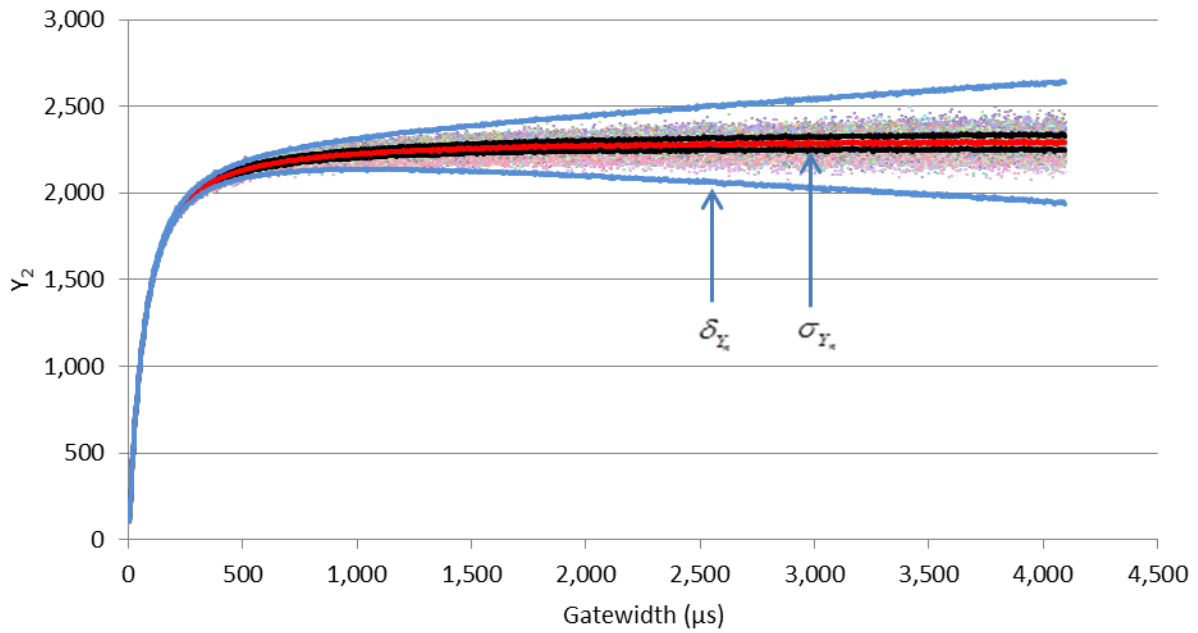


Figure 3. Estimation of Y_2 parameter for each gatewidth for a simulation of a 4.5 kg sphere of plutonium. The red center line is the average value for Y_2 for each gatewidth while the black line is the uncertainty calculated by σ_{Y_2} for each gatewidth. The blue divergent line is the uncertainty as calculated by δ_{Y_2} for each gatewidth.

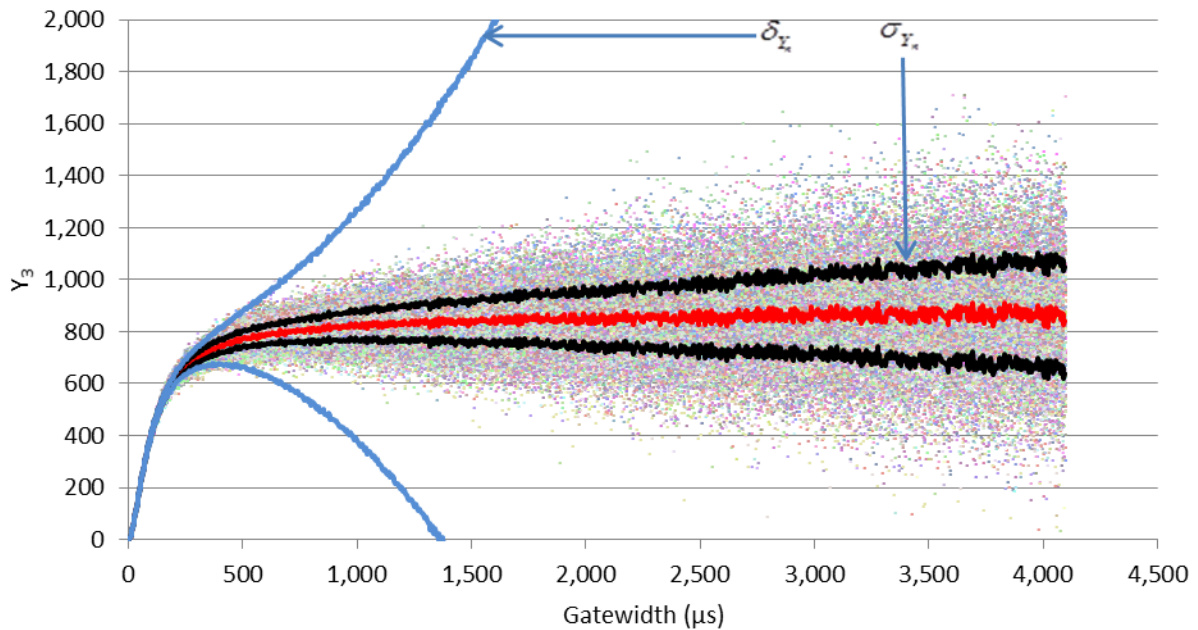


Figure 4. Estimation of Y_3 parameter for each gatewidth for a simulation of a 4.5 kg sphere of plutonium. The red center line is the average value for Y_3 for each gatewidth while the black line is the uncertainty calculated by σ_{Y_3} for each gatewidth. The blue divergent line is the uncertainty as calculated by δ_{Y_3} for each gatewidth.

A better evaluation of the uncertainty is to bin the data into a histogram and examine how the calculated uncertainties compare with the sample standard deviation. The Y_n parameters for the 2,048 μs gate were binned into histograms and these results are plotted in Figure 5, Figure 6, and Figure 7. From these figures we can again see that the uncertainty calculated by σ_{Y_n} is in much better agreement with the sample standard deviation than the uncertainty calculated by δ_{Y_n} .

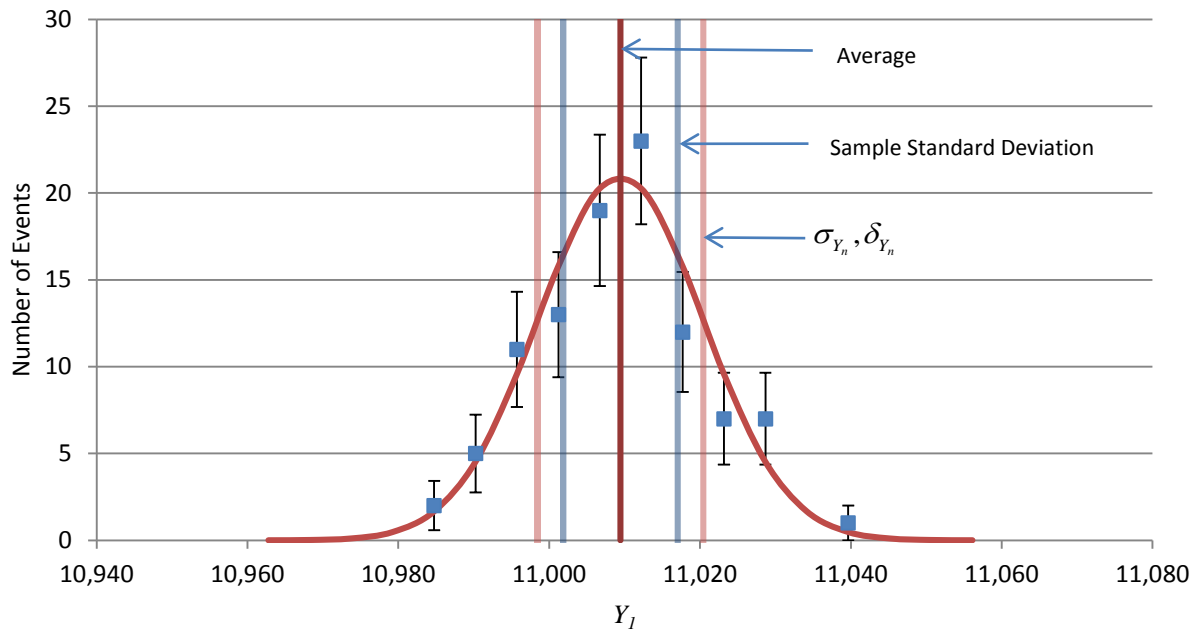


Figure 5. A histogram of the Y_I values for each simulation of a 4.5 kg sphere of Pu for the 2,048 μs gatewidth. Also plotted are the sample standard (blue lines) and the uncertainty calculated by σ_{Y_i} (red lines). Note: for Y_I , $\sigma_{Y_i} = \delta_{Y_i}$.

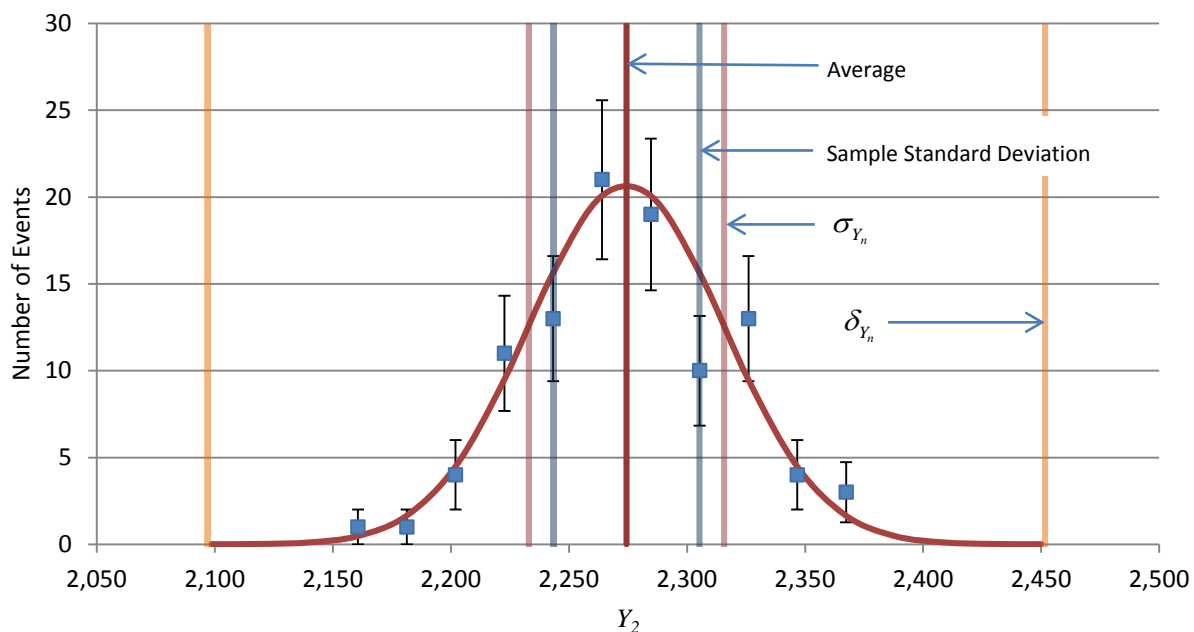


Figure 6. A histogram of the Y_2 values for each simulation of a 4.5 kg sphere of Pu for the 2,048 μ s gatewidth. Also plotted are the sample standard deviation (blue lines), the uncertainty calculated by σ_{Y_2} (red lines), and the uncertainty calculated by δ_{Y_2} (orange lines).

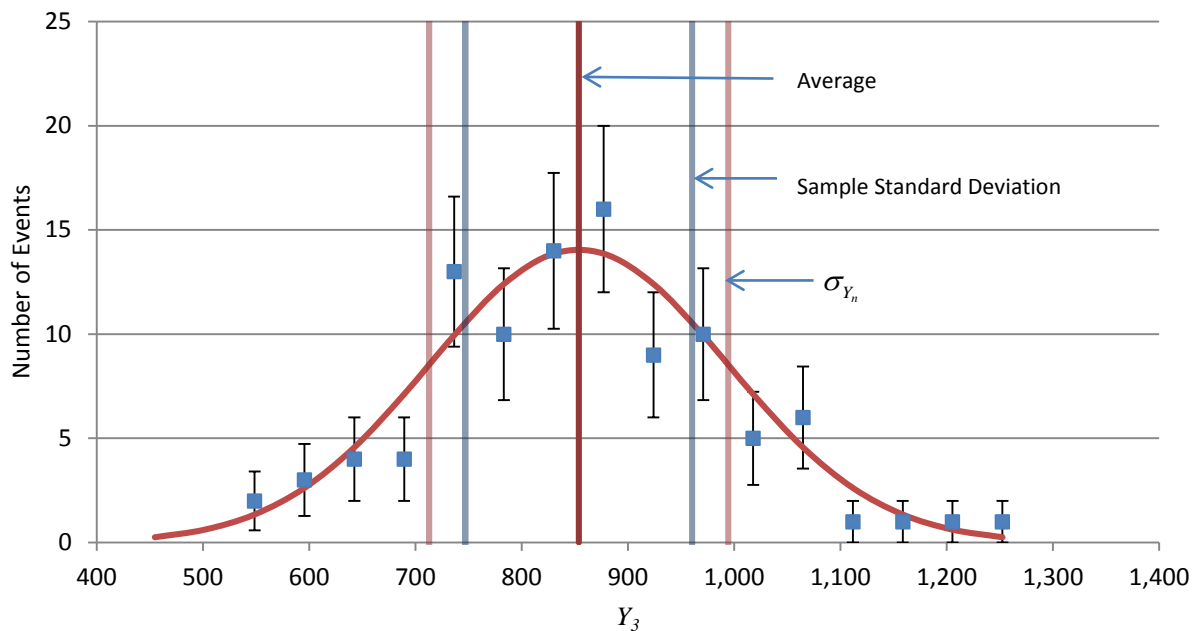


Figure 7. A histogram of the Y_3 values for each simulation of a 4.5 kg sphere of Pu for the 2,048 μ s gatewidth. Also plotted are the sample standard deviation (blue lines), and the uncertainty calculated by σ_{Y_3} (red lines). The uncertainty calculated by δ_{Y_3} is outside the scale plotted.

Comparison with Theory

The first four rates of the 100 simulations were fitted with the Hage-Cifarelli model.

The Levenberg-Marquardt (LM) method was initially used to fit the data [15] using χ^2 as the minimization parameter. It was found that the LM method would occasionally result in a bad fit and it appears there is a local minimum in which the LM method cannot escape from. This appears to be in agreement with the results found by Okowita [12]. The Nelder-Mead method, commonly referred to as amoeba [15], was implemented next and resulted in better fits when using χ^2 as the minimization parameter. The amoeba method was able to move out of the local minimum to the global minimum. The minimization parameter is

$$\chi^2 = \sum_{k=0}^K \left(\frac{Y_{nk} - Y_{nk-Fit}}{\sigma_{Y_{nk}}} \right)^2. \quad (42)$$

The equations used for fitting are

$$Y_1 = R_1 \omega_1(\tau), \quad (43)$$

$$Y_2 = R_2 \omega_2(\tau), \quad (44)$$

$$Y_3 = R_3 \omega_3(\tau), \text{ and} \quad (45)$$

$$Y_4 = R_4 \omega_4(\tau). \quad (46)$$

Where

$$\omega_1(\tau) = 1, \quad (47)$$

$$\omega_2(\tau) = 1 - \frac{1 - e^{-\lambda\tau}}{\lambda\tau}, \quad (48)$$

$$\omega_3(\tau) = 1 - \frac{1}{2\lambda\tau} (3 - 4e^{-\lambda\tau} + e^{-2\lambda\tau}), \text{ and} \quad (49)$$

$$\omega_4(\tau) = 1 - \frac{11 - 2e^{-3\lambda\tau} + 9e^{-2\lambda\tau} - 18e^{-\lambda\tau}}{6\lambda\tau}. \quad (50)$$

The parameters R_1 , R_2 , R_3 , and R_4 are termed the singles, doubles, triples, and quad rates respectively. The parameter λ is the inverse neutron diffusion time. That is the average time it takes for a neutron once it is created to be detected in the neutron detector. The resulting fits for a single simulation are shown in Figure 8, Figure 9, Figure 10, and Figure 11. The fits show good agreement with the data when using σ_{Y_n} and this is evident because the reduced chi-squared for the fits to the doubles, triples, and quads are all around one.

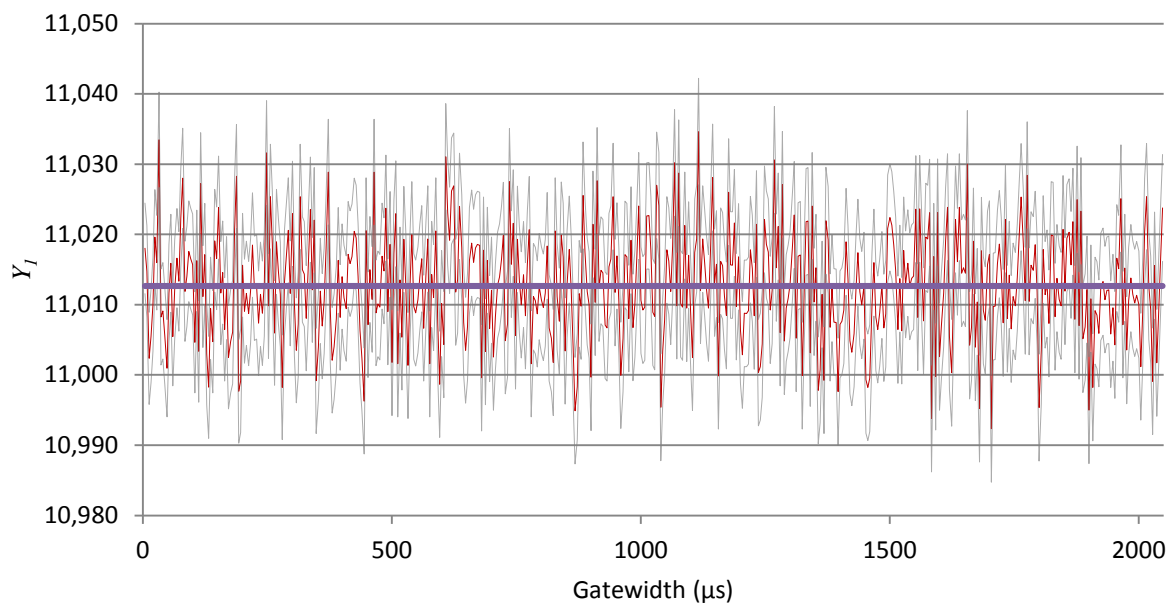


Figure 8. The Y_1 parameter as a function of gatewidth fitted for a simulation of a 4.5 kg sphere of Pu. The reduced χ^2 for this fit is 1.00.

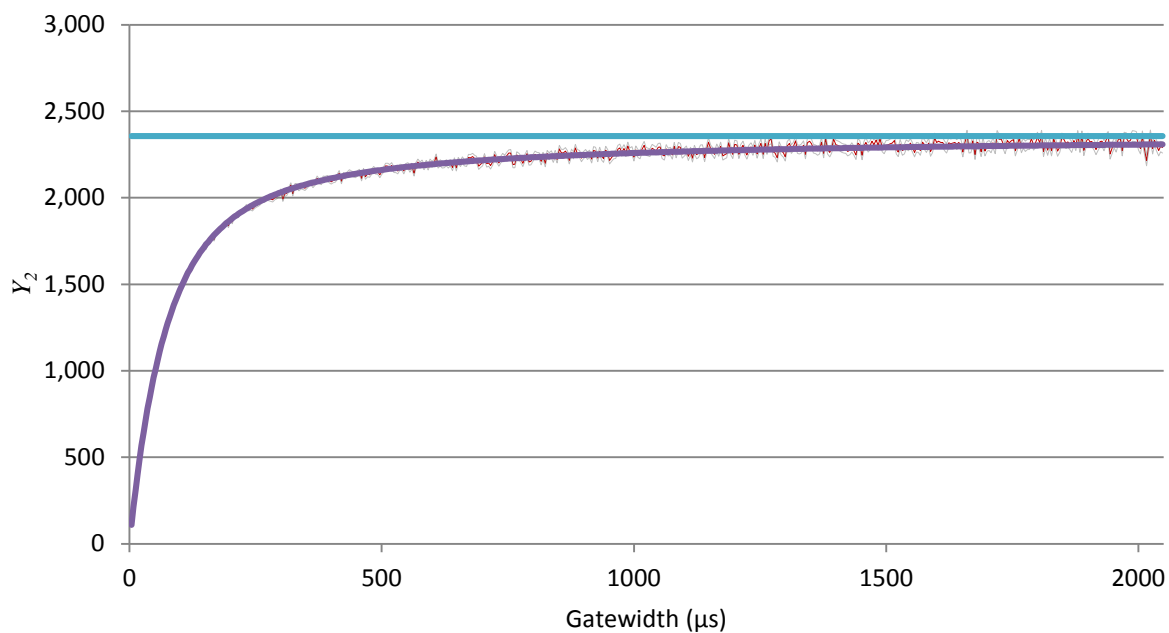


Figure 9. The Y_2 parameter as a function of gatewidth fitted for a simulation of a 4.5 kg sphere of Pu. The reduced χ^2 for this fit is 1.08.

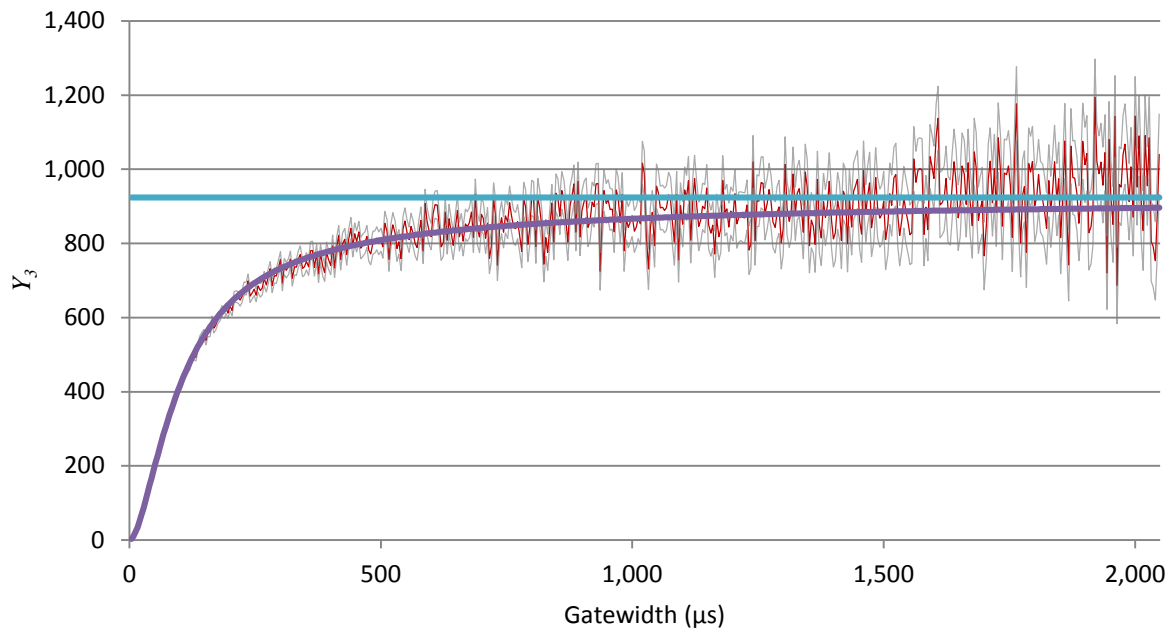


Figure 10. The Y_3 parameter as a function of gatewidth fitted for a simulation of a 4.5 kg sphere of Pu. The reduced χ^2 for this fit is 1.06.

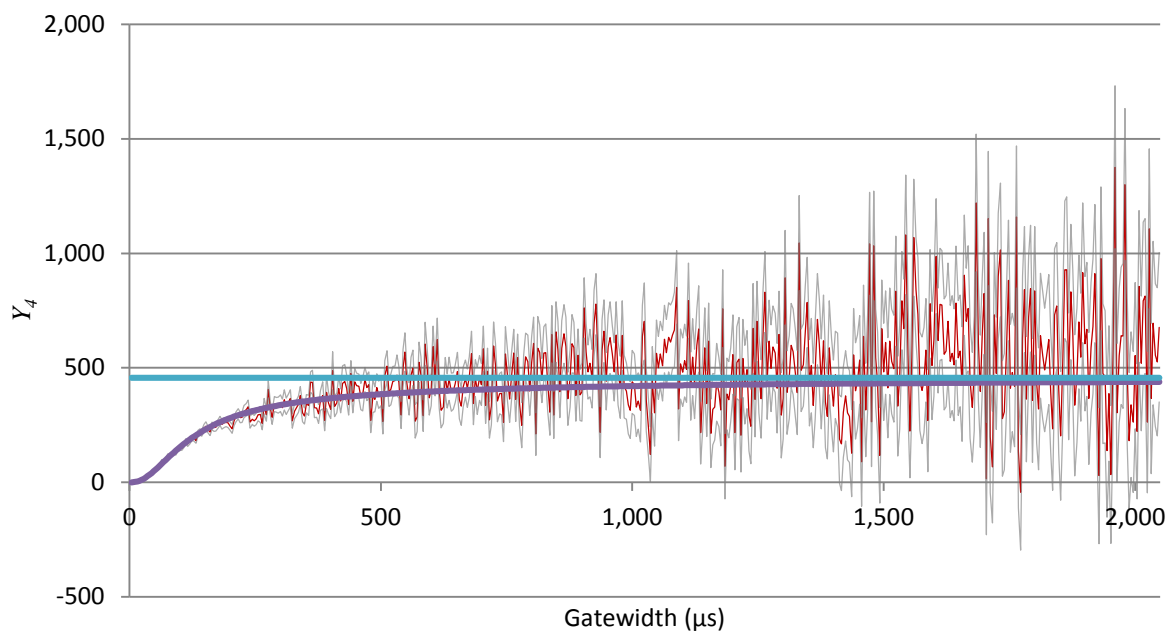


Figure 11. The Y_4 parameter as a function of gatewidth fitted for a simulation of a 4.5 kg sphere of Pu. The reduced χ^2 for this fit is 1.19.

Highly Enriched Uranium System

It has been demonstrated that σ_{Y_n} works well for high count rate systems. Low count rate systems, however, have significantly less number of counts and confirmation that this method works for low count rate systems is examined next.

One hundred (100) monte-carlo simulations were performed to emulate a 40 kg sphere of highly enriched uranium. This data was processed the same way as the previous plutonium simulations. The uncertainty was only calculated using the propagation of uncertainty (σ_{Y_n}) and the results are plotted below in Figure 12, Figure 13, and Figure 14. The comparisons of the fits to the data are presented in Figure 15, Figure 16, Figure 17, and Figure 18. The equations for the uncertainty are again in good agreement with the simulated data.

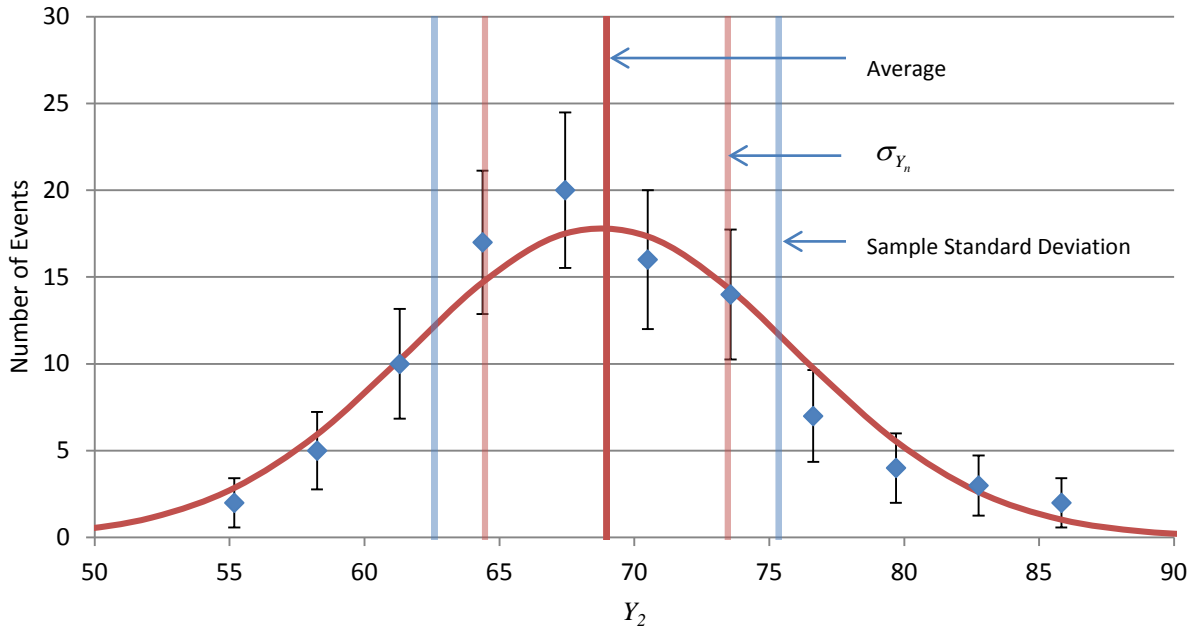


Figure 12. A histogram of the Y_I values for each simulation of a 40 kg sphere of highly enriched uranium for the 2,048 μ s gatewidth. Also plotted are the sample standard deviation (blue lines) and the uncertainty calculated by σ_{Y_n} (red lines).

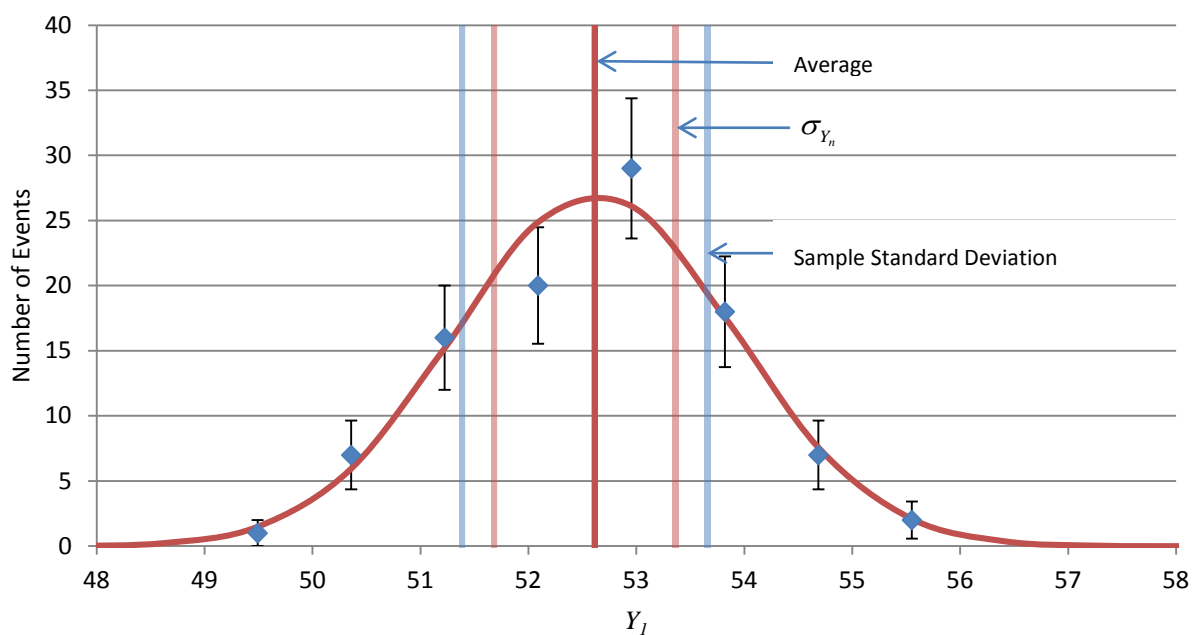


Figure 13. A histogram of the Y_2 values for each simulation of a 40 kg sphere of highly enriched uranium for the 2,048 μ s gatewidth. Also plotted are the sample standard deviation (blue lines) and the uncertainty calculated by σ_{Y_2} (red lines).

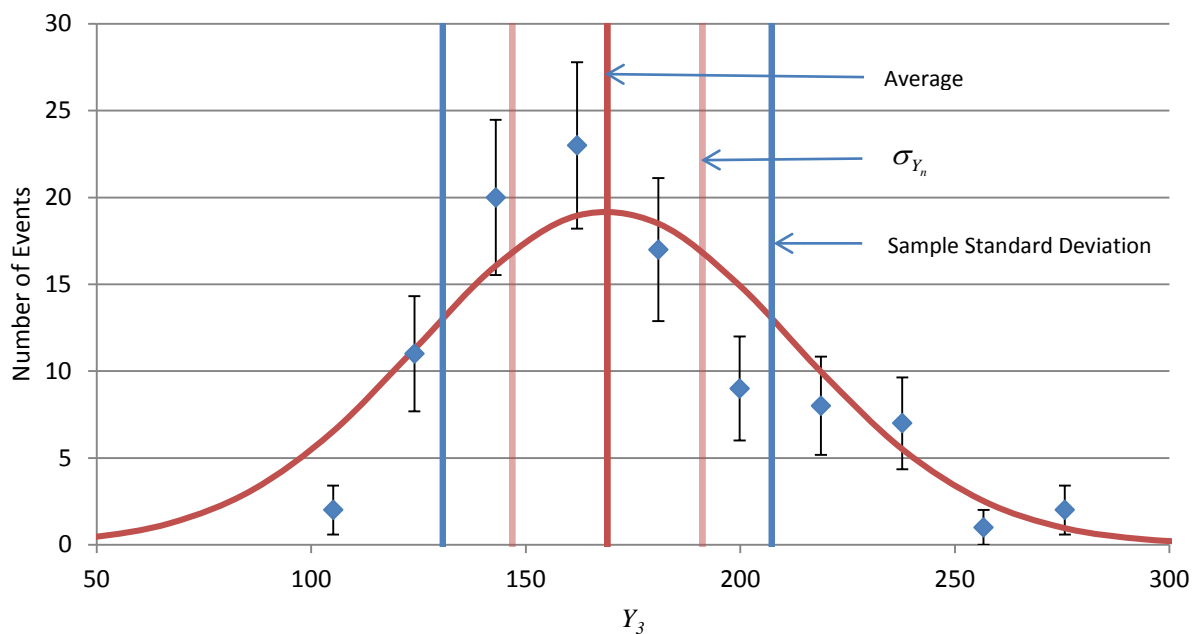


Figure 14. A histogram of the Y_3 values for each simulation of a 40 kg sphere of highly enriched uranium for the 2,048 μ s gatewidth. Also plotted are the sample standard deviation (blue lines) and the uncertainty calculated by σ_{Y_3} (red lines).

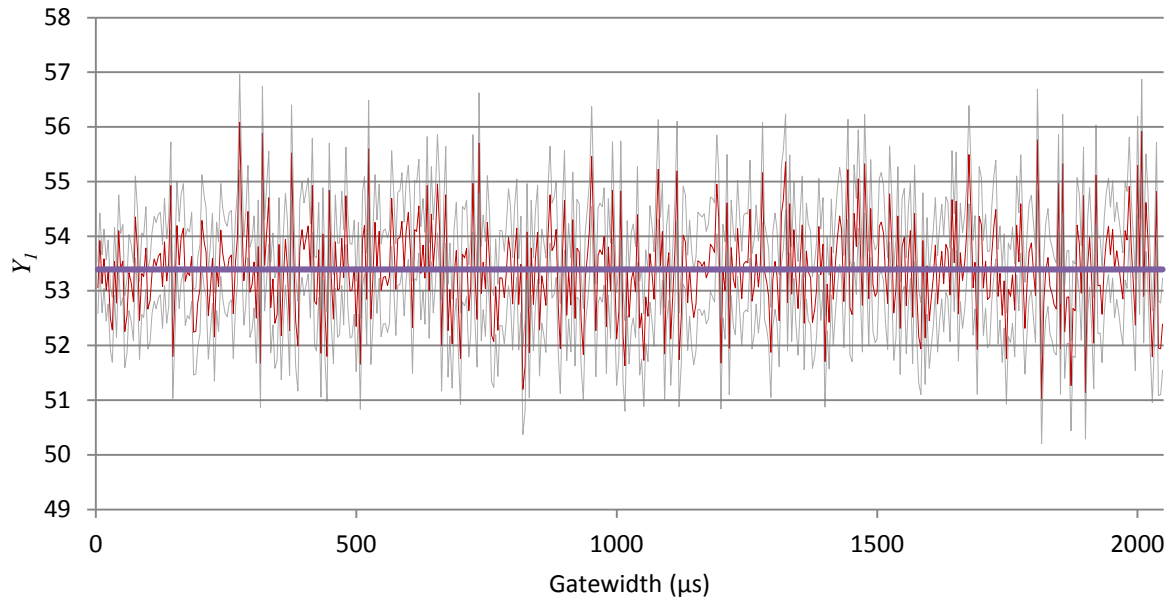


Figure 15. The Y_I parameter as a function of gatewidth fitted for a simulation of a 40 kg sphere of highly enriched uranium. The reduced chi-squared for this fit is 1.00.

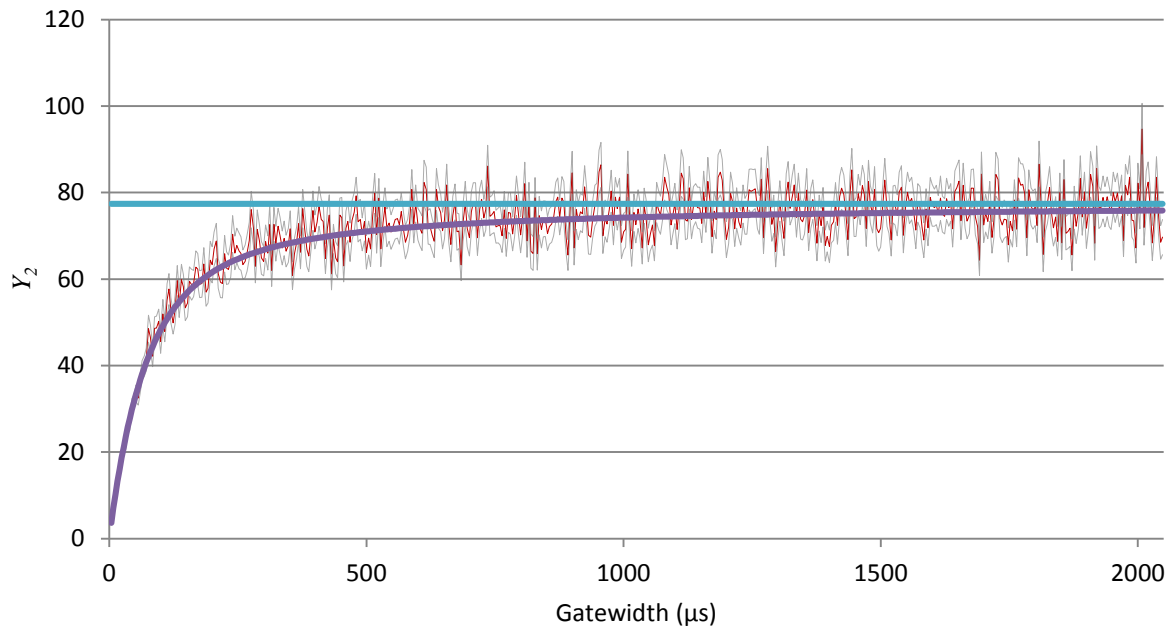


Figure 16. The Y_2 parameter as a function of gatewidth fitted for a simulation of a 40 kg sphere of highly enriched uranium. The reduced chi-squared for this fit is 1.19.

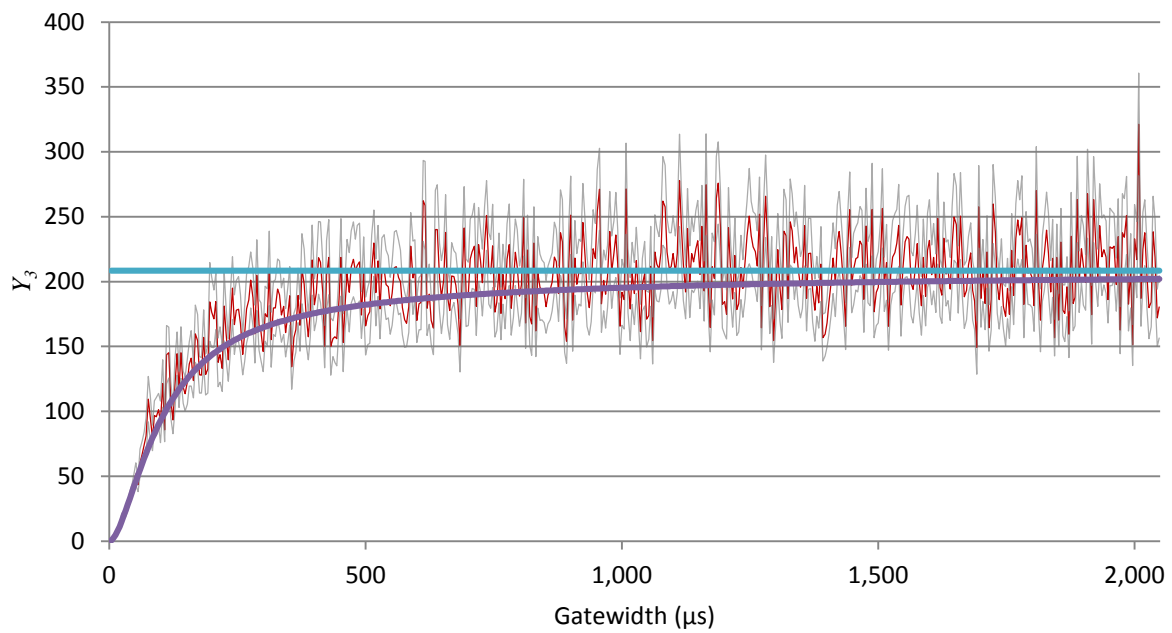


Figure 17. The Y_3 parameter as a function of gatewidth fitted for a simulation of a 40 kg sphere of highly enriched uranium. The reduced chi-squared for this fit is 1.44.

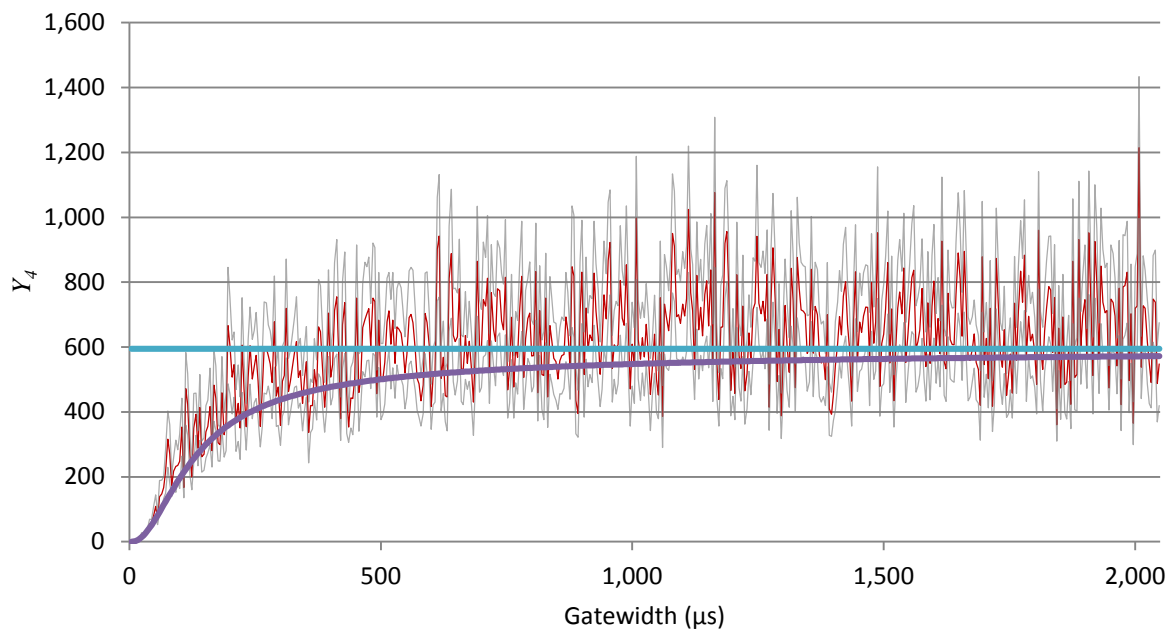


Figure 18. The Y_4 parameter as a function of gatewidth fitted for a simulation of a 40 kg sphere of highly enriched uranium. The reduced chi-squared for this fit is 1.85.

Behavior of uncertainty

The previous uncertainties were calculated where the number of gates changed depending upon the total count time. This section will compare the behavior of the uncertainty if the total number of gates is kept constant.

It is easy to take the fits of the values for the singles, double, triples and quads and invert the equations to get the uncertainties.

These equations are

$$\Delta Y_1 = \frac{\sqrt{2R_2\omega_2\tau + R_1\tau}}{\sqrt{N-1} \times \tau}, \text{ and} \quad (51)$$

$$\Delta Y_2 = \frac{\sqrt{6R_1^2\omega_2R_2\tau^3 - \frac{3}{2}R_1^5\tau^5 - 6R_1^3\omega_2R_2\tau^4 - 6R_1(\omega_2R_2)^2\tau^3 + 2(\omega_2R_2)^2\tau^2 + 6\omega_4R_4\tau + 2R_1\omega_2R_2\tau^2 + 6\omega_3R_3\tau + \frac{1}{2}R_1^2\tau^2 + \omega_2R_2\tau}}{\sqrt{N-1} \times \tau}. \quad (52)$$

The average of the moments of the 100 plutonium simulations were calculated and plotted against the sample uncertainty for Y_1 and Y_2 . This data is plotted in Figure 19 and Figure 20, respectively. For these figures, the number of gatewidths was dependent upon the measurement time. The number of gates generated were

$$\text{number of Gates} = 0.8 \frac{\text{Total Count Time}}{\text{Gatewidth}}$$

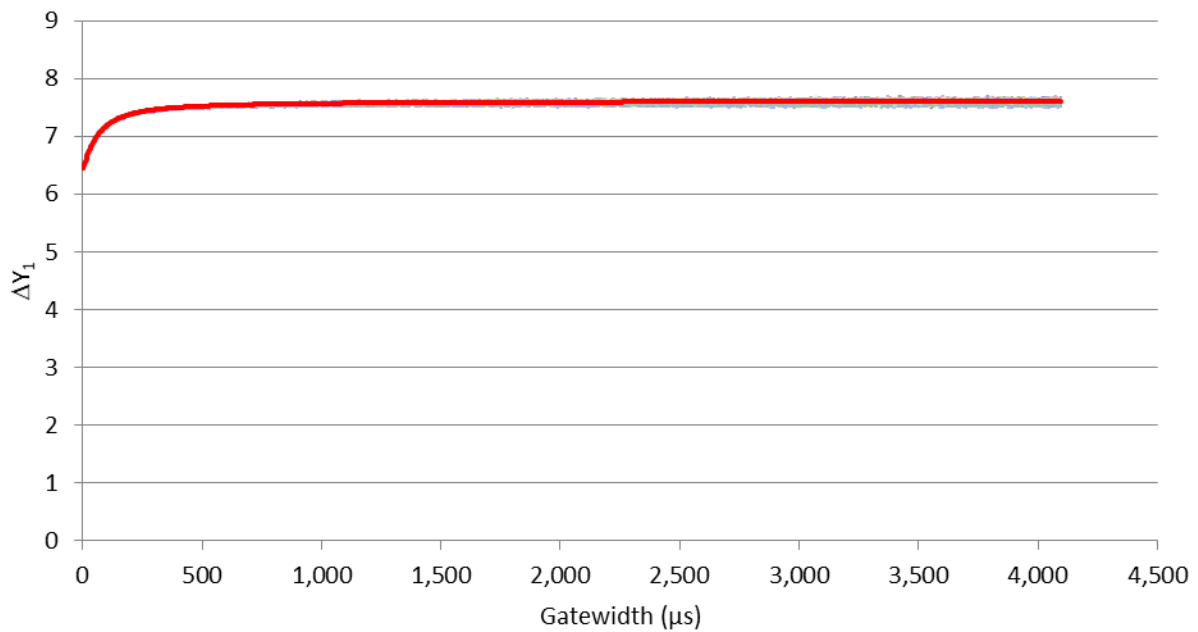


Figure 19. The expected uncertainty for Y_1 as a function of gatewidth plotted on top of the sample uncertainties. The number of gatewidths is not the same for each gatewidths.

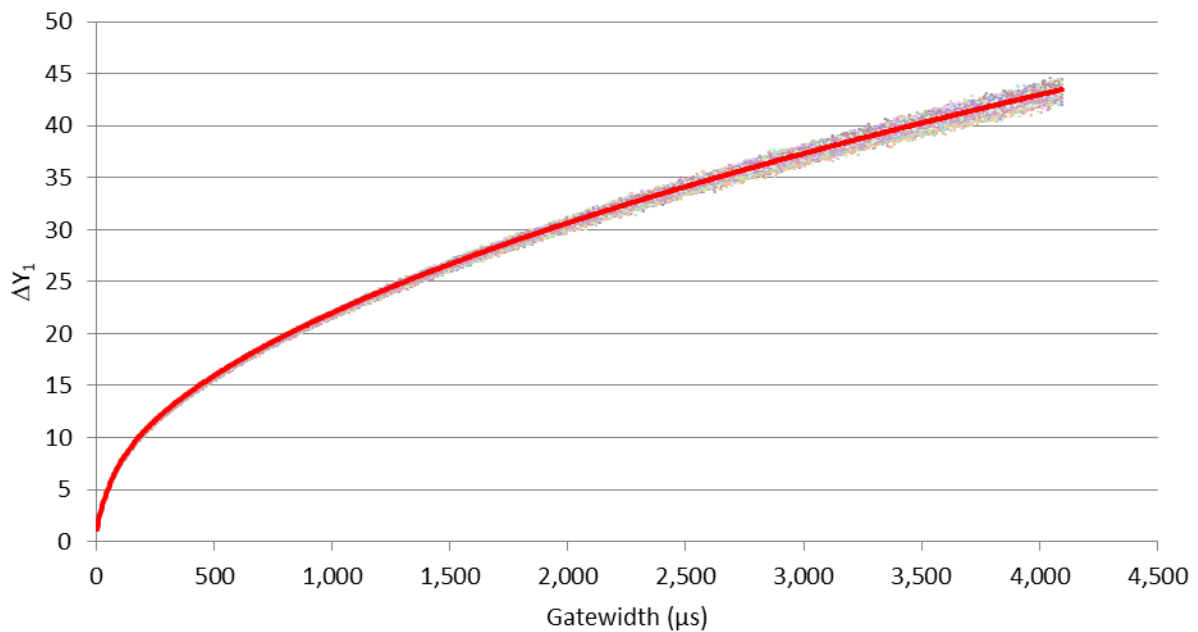


Figure 20. The expected uncertainty for Y_2 as a function of gatewidth plotted on top of the sample uncertainties. The number of gatewidths is not the same for each gatewidths.

Constant Number of Gates for Each Gatewidth

If the total number of gates for each Feynman histogram is kept constant the shape of the uncertainty curves as a function of gatewidth changes. This can be seen Figure 21 and Figure 22. The plots demonstrate that for the singles rate, the uncertainty increases significantly for small gatewidths when the number of gates is kept constant. Alternatively the uncertainty is relatively constant when the number of gates is proportional to the count time. This trend changes for Y_2 where the uncertainty increases when the number of gates is proportional to the count time but is relatively constant when the number of gates is constant. The triples rate was not examined because this would require fitting the quintuplet and sextuplet parameters and the derivation of these parameters is outside the scope of this paper.

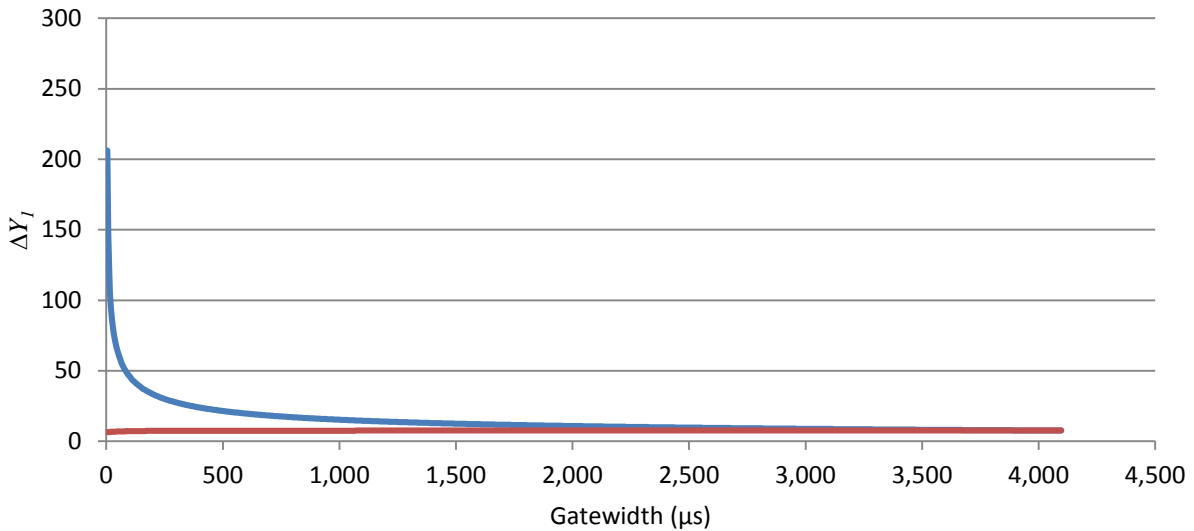


Figure 21. The expected uncertainties for Y_I when the number of gates is kept constant (top blue curve) and when the number of gates changes is 80% of the total count time over the gatewidth (lower red curve).

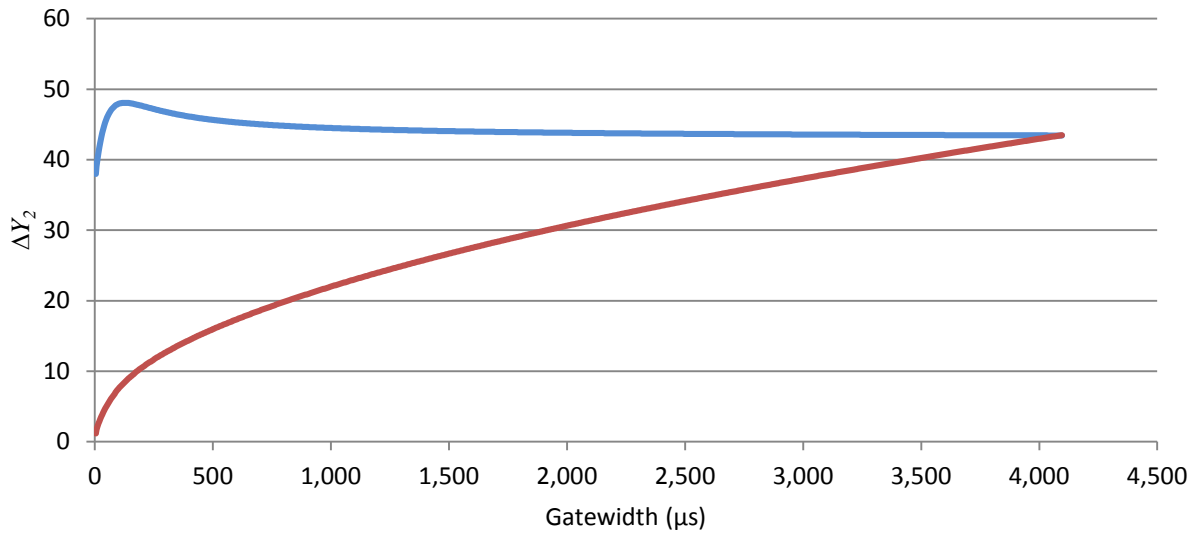


Figure 22. The expected uncertainties for Y_2 when the number of gates is kept constant (top blue curve) and when the number of gates changes is 80% of the total count time over the gatewidth (lower red curve).

Uncertainty for Fraction Y_n Parameters

There is a variation of the Y_n parameters, the fractional Y_n parameters, or Y_{nf} . The second, third, and fourth fractional parameters are

$$Y_{2f} = \frac{Y_2}{Y_1}, \quad (53)$$

$$Y_{3f} = \frac{Y_3}{Y_1}, \text{ and} \quad (54)$$

$$Y_{4f} = \frac{Y_4}{Y_1}. \quad (55)$$

Following the same methods outlined above by propagating the uncertainty, the uncertainties are

$$\sigma_{Y_{2f}} = \frac{\sqrt{\frac{1}{2} \overline{m_2} + \frac{1}{4} \overline{m_1} - \frac{1}{4} \overline{m_1}^2 + 2 \frac{\overline{m_2}^2}{\overline{m_1}} - \frac{\overline{m_2}}{\overline{m_1}} + 2 \frac{\overline{m_2}^3}{\overline{m_1}^4} - 3 \frac{\overline{m_2}^2}{\overline{m_1}^3} + 6 \frac{\overline{m_4}}{\overline{m_1}^2} + 6 \frac{\overline{m_3}}{\overline{m_1}^2} + \frac{\overline{m_2}}{\overline{m_1}} - 3 \frac{\overline{m_3}}{\overline{m_1}} - 6 \frac{\overline{m_2} \overline{m_3}}{\overline{m_1}^3}}}{\sqrt{N-1}}, \quad (56)$$

$$\sigma_{Y_{3f}} = \frac{\frac{4}{9}\overline{m_1^{-3}} - \overline{m_2^{-2}} - \frac{4}{9}\overline{m_1^{-4}} + \overline{m_2} + \frac{26}{3}\overline{m_3} + \frac{34}{3}\overline{m_4} - 8\frac{\overline{m_3 m_4}}{\overline{m_1^{-3}}} - \frac{8}{3}\frac{\overline{m_3 m_2}}{\overline{m_1}} + 2\frac{\overline{m_3^{-2} m_2}}{\overline{m_1^{-4}}} - \frac{8}{3}\overline{m_2 m_1} - 4\overline{m_1 m_3} + \frac{20}{9}\overline{m_2 m_1^{-2}} + 12\frac{\overline{m_4}}{\overline{m_1^2}} + \frac{\overline{m_3}}{\overline{m_1^2}} - 6\frac{\overline{m_3}}{\overline{m_1}} + 4\frac{\overline{m_2 m_3}}{\overline{m_1^{-2}}} - 5\frac{\overline{m_3}}{\overline{m_1^3}} + 6\frac{\overline{m_3^{-2}}}{\overline{m_1^2}} + 20\frac{\overline{m_6}}{\overline{m_1^2}} + 30\frac{\overline{m_5}}{\overline{m_1^2}} - 20\frac{\overline{m_5}}{\overline{m_1}} - 24\frac{\overline{m_4}}{\overline{m_1}}}{\sqrt{N-1}}, \text{ and}$$

$$\sigma_{Y_{4f}} = \frac{6 \frac{\overline{m_2 m_4 m_3}}{\overline{m_1^3}} + \overline{m_3} + 24 \overline{m_4} + 50 \overline{m_6} + 70 \overline{m_5} - 2 \overline{m_2^2} - \overline{m_3^2} + \frac{\overline{m_2^3}}{\overline{m_1^2}} + \frac{29}{4} \overline{m_2^2 m_1} - \frac{31}{4} \overline{m_2^2 m_1^2} - \frac{9}{2} \overline{m_2 m_1^3} + \frac{33}{8} \overline{m_2 m_1^4} + \frac{7}{4} \frac{\overline{m_2^4}}{\overline{m_1^2}} - \frac{\overline{m_2^3}}{\overline{m_1}} + 12 \overline{m_4 m_1^2} - 7 \frac{\overline{m_4^2}}{\overline{m_1^3}} + 8 \frac{\overline{m_4^2}}{\overline{m_1^2}} + \frac{1}{2} \frac{\overline{m_2^5}}{\overline{m_1^4}} - \frac{7}{4} \frac{\overline{m_2^4}}{\overline{m_1^3}} + 140 \frac{\overline{m_7}}{\overline{m_1^2}} + 70 \frac{\overline{m_8}}{\overline{m_1^2}} - 6 \overline{m_1^3 m_3} - \frac{55}{2} \overline{m_1 m_5} - 120 \frac{\overline{m_6}}{\overline{m_1}} - 70 \frac{\overline{m_7}}{\overline{m_1}} - 6 \overline{m_1 m_3} + \overline{m_2 m_1^2} - \frac{57}{2} \overline{m_1 m_4} - 18 \overline{m_2 m_3} - 17 \overline{m_2 m_4} + 90 \frac{\overline{m_6}}{\overline{m_1^2}} + 20 \frac{\overline{m_5}}{\overline{m_1^2}} + \frac{21}{2} \overline{m_1^2 m_3} - 60 \frac{\overline{m_5}}{\overline{m_1}} - 8 \frac{\overline{m_4}}{\overline{m_1}} + \frac{\overline{m_4}}{\overline{m_1^2}} + 6 \frac{\overline{m_3 m_2}}{\overline{m_1}} + 6 \frac{\overline{m_3 m_4}}{\overline{m_1^2}} + \frac{5}{2} \overline{m_2^3} + \frac{9}{16} \overline{m_1^5} - \frac{9}{16} \overline{m_1^6} - 30 \frac{\overline{m_2 m_6}}{\overline{m_1^2}} - 4 \frac{\overline{m_2^2 m_3}}{\overline{m_1}} + 26 \frac{\overline{m_2 m_4}}{\overline{m_1}} - 3 \frac{\overline{m_2^3 m_3}}{\overline{m_1^3}} + 7 \frac{\overline{m_4 m_2^2}}{\overline{m_1^3}} - 12 \frac{\overline{m_2 m_4}}{\overline{m_1}} + 3 \frac{\overline{m_2^2 m_3}}{\overline{m_1^2}} + 2 \frac{\overline{m_4^2 m_2}}{\overline{m_1^4}} + \frac{29}{2} \overline{m_1 m_2 m_3} - 6 \frac{\overline{m_3 m_4}}{\overline{m_1}} - 2 \frac{\overline{m_2^2 m_4}}{\overline{m_1^2}} - 2 \frac{\overline{m_4 m_2^3}}{\overline{m_1^4}} + 30 \frac{\overline{m_2 m_5}}{\overline{m_1}} - 10 \frac{\overline{m_4 m_5}}{\overline{m_1^3}} + 5 \frac{\overline{m_2^2 m_5}}{\overline{m_1^3}} - 40 \frac{\overline{m_2 m_5}}{\overline{m_1^2}}}{\sqrt{N-1}}. \quad (58)$$

Finally, there is the Y_m parameter presented by Robba [3] which is

$$Y_M = \frac{\overline{C_2}}{\overline{C_1}} - \overline{C_1} - 1 = 2Y_{2f}. \quad (59)$$

And the uncertainty is

$$\sigma_{Y_M} = \frac{\sqrt{2 \frac{\overline{C_2}^2}{\overline{C_1}^2} + \frac{\overline{C_2}^3}{\overline{C_1}^4} + \overline{C_2} - \overline{C_1}^2 + \frac{\overline{C_4}}{\overline{C_1}^2} - 2 \frac{\overline{C_2} \overline{C_3}}{\overline{C_1}^3} - 2 \frac{\overline{C_3}}{\overline{C_1}}}}{\sqrt{N-1}} = 2\sigma_{Y_{2f}}. \quad (60)$$

The reduced χ^2 of fits using the above equations are presented in Table 5. The reduced chi-squared is again close to one suggesting that these equations for uncertainty are good estimators for their associated parameters.

Table 5. The reduced chi-squared of curve fits for the associated fractional Y_f and Y_M parameters.

Parameter	Reduced chi-squared of fits using the associated uncertainty terms.
Y_{2f}	1.09
Y_{3f}	1.09
Y_{4f}	1.14
Y_M	1.09

Conclusion

Two separate methods for calculating the uncertainty in the parameters used for estimating the multiplicity rates used in the Hage-Cifarelli formalism were evaluated. It was demonstrated that the standard propagation of uncertainty for the Y_n parameters (σ_{Y_n} - equations (28) through (41)) yield better estimates on the uncertainty than the difference of values. When fitting the resulting Y_n parameters and using the reduced χ^2 minimization parameter, the fits are reasonable and the reduced chi-squared is close to one. Finally, the uncertainty parameters are also presented for the fractional Y_n and the Y_M parameters.

¹ D. Cifarelli, W. Hage, "Models for a Three-Parameter Analysis of Neutron Signal Correlation Measurements for Fissile Material Assay," Nucl. Inst. Meth. A251, 550-563 (1986).

² Wikipedia, the free encyclopedia. "Moment (mathematics)." http://en.wikipedia.org/wiki/Moment_%28mathematics%29. Jan 1 (2015).

³ A. Robba, E. Dowdy, H. Atwater "Neutron Multiplication Measurements Using Moments of the Neutron Counting Distribution." Nucl. Inst. Meth 215. 473-479 (1983).

⁴ M. Smith-Nelson, et al. "Neutron Specialist Handbook and Informational Text." Los Alamos National Laboratory, LA-UR-07-6170 (2007).

⁵ T. Burr and M. Smith-Nelson, "Experimental Verification of Variance Results for the Second and Third Reduced Factorial Sample Moments in Neutron Multiplicity Counting." IJRRAS, Vol 13, Issue 2 (2012).

⁶ T. Cutler, M Smith-Nelson, and J. Hutchinson, "Deciphering the Binning Method Uncertainty in Neutron Multiplicity Measurements." Los Alamos National Laboratory, LA-UR-14-23374 (May 2014).

⁷ M. Krick, W. Geist, and D. Mayo. "A Weighted Point Model for the Thermal Neutron Multiplicity Assay of High-Mass Plutonium Samples." Los Alamos National Laboratory, LA-14157 (Oct 2005).

⁸ B. Richard, and J. Hutchinson. "Nickel-Reflected Plutonium-Metal-Sphere Subcritical Measurements." FUND-NCERC-PU-HE3-MULT-001 (2014).

⁹ J. Verbeke. "Determination of the standard deviation on multiplication based on count distributions." Lawrence Livermore National Laboratory. LLNL-TR-448118 (August 2010).

¹⁰ T. Burr, and K. Butterfield. "Variance Results for the Second and Third Reduced Moments in Neutron Counting for Randomly Triggered or Signal Triggered Counting Gates." Nucl. Inst. Meth. A 594, 257-265 (2008).

¹¹ J. Mattingly. "Propagation of Uncertainty in the Feynman-Y." Personal communication (2013).

¹² A. Okowita, and J. Mattingly. "Analysis of the Feynman Variance to Mean Ratio Using Nonlinear Regression." Dept. of Nuclear Engineering, North Carolina State University. Presented at Institute for Nuclear Materials Management (2012).

¹³ Maple (ver 14.0). Maplesoft, a division of Waterloo Maple Inc., Waterloo, Ontario (2010).

¹⁴ S. Nolen. "The Chain-Length Distribution in Subcritical Systems." Los Alamos National Laboratory, LA-13721-T (June 2000).

¹⁵ W. Press, S. Teukolsky, W. Vetterling, and B. Flannery. "Numerical Recipes in C. The Art of Scientific Computing, Second Edition." Cambridge, United Kingdom. Cambridge University Press (1999).